Saturation effects in the sub-Doppler spectroscopy of cesium vapor confined in an extremely thin cell

C. Andreeva, S. Cartaleva,* and L. Petrov
Institute of Electronics, Bulgarian Academy of Sciences, 72 Tzarigradsko Shosse Boulevard, 1784 Sofia, Bulgaria

S. M. Saltiel
Faculty of Physics, Sofia University, 5 J. Bourchier Boulevard, 1164 Sofia, Bulgaria

D. Sarkisyan and T. Varzhapetyan
Institute for Physical Research, NAS of Armenia, Ashtarak-2, Armenia

D. Bloch and M. Ducloy
Laboratoire de Physique des Lasers UMR 7538 du CNRS, Université Paris-13, F-93430 Villetaneuse, France
(Received 10 June 2006; revised manuscript received 23 March 2007; published 31 July 2007)

Saturation effects affecting absorption and fluorescence spectra of an atomic vapor confined in an extremely thin cell (cell thickness $L<1$ μm) are investigated experimentally and theoretically. The study is performed on the D_2 line ($\lambda=852$ nm) of Cs and concentrates on the two situations $L=\lambda/2$ and $L=\lambda$, the most contrasted ones with respect to the length dependence of the coherent Dicke narrowing. For $L=\lambda/2$, the Dicke-narrowed absorption profile simply broadens and saturates in amplitude when increasing the light intensity, while for $L=\lambda$, sub-Doppler dips of reduced absorption at the line-center appear on the broad absorption profile. For a fluorescence detection at $L=\lambda$, saturation induces narrow dips, but only for hyperfine components undergoing a population loss through optical pumping. These experimental results are interpreted with the help of the various existing models and are compared with numerical calculations based upon a two-level modeling that considers both a closed and an open system.

DOI: 10.1103/PhysRevA.76.013837 PACS number(s): 42.62.Fi, 42.50.Gy, 42.50.Ct

I. INTRODUCTION

High-resolution spectroscopy of atoms confined in a thin cell is promising for the investigation of complex spectra of atoms and molecules. When irradiating a 10–1000 μm thin cell under normal incidence, the transmission spectrum of a single light beam had revealed tiny sub-Doppler features, nevertheless allowing the resolution of the hyperfine structure (hfs) of alkali atoms resonances [1–3]. Indeed, the atoms travel wall-to-wall and resonantly interact with light according to a transient regime, yielding an enhanced response for atoms with longer interaction time, i.e., for those atoms insensitive to a Doppler shift. Recently, the extension to a technology of extremely thin cell (ETC, thickness $L<1$ μm) [4] has shown that these sub-Doppler resonances become easily observed and can be a dominant effect, even in the absence of a frequency modulation (FM) technique. With these ETCs, an even narrower fluorescence spectrum can also be detected, showing that transmission and fluorescence behave differently. For the transmission spectrum, it was shown that one observes a maximal coherent sub-Doppler Dicke narrowing [5] for a cell length $L=\lambda/2$, with periodic revivals at $(2n+1)\lambda/2$ [2,6], while for $L=\lambda$ (or $n\lambda$), the local coherent atomic response is phase-mismatched all over the ETC, making the sub-Doppler features vanishing and only allowing a residual Doppler-broadened response. This length-dependent narrowing has no equivalent in the detection of an incoherent process such as the fluorescence [7], whose narrow features simply originate from the enhancement of the contribution of those atoms whose velocity allows for a long interaction time. This leads to a behavior that is monotonic with the cell thickness. These features of sub-Doppler transmission and fluorescence in ETCs were demonstrated in the linear regime of interaction (with respect to intensity), allowing, for example, the experimental determination of transition probabilities of the respective hfs components [8].

The detailed mechanisms for these sub-Doppler features are known to be complex because, depending upon the irradiating intensity, a coherent linear regime [2] and an (incoherent) nonlinear regime of optical pumping had already been distinguished for the absorption in relatively long cells ($L\geqslant 10$ μm) [1–3]. As long as the atomic system can be described in a two-level frame, various treatments for transmission experiments were developed in an asymptotic regime relative to the irradiating intensity [1–3,9], up to a full analytical formal expansion [10]. For ETCs, these high-intensity effects become even more complex, with respect to the interplay between the interferometric dependence associated to the Dicke narrowing, and the velocity-dependent efficiency of saturation mechanisms.

In this paper, we present an experimental and theoretical study of the intensity effects in an ETC. For simplicity, we restrict our experiments to the two cases $L=\lambda/2$ and $L=\lambda$, the most important ones with respect to the periodicity of the Dicke coherent narrowing. An additional simplicity for this restriction is that it allows one to neglect some of the Fabry-Perot effects intrinsic to ETCs, namely the mixing of trans-

*stefka-c@ie.bas.bg

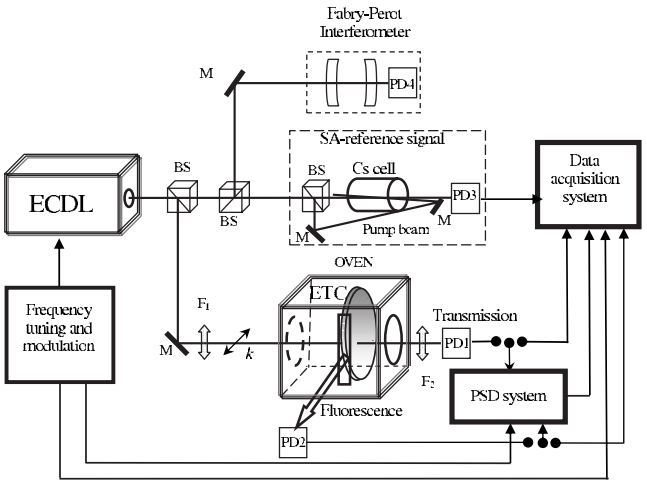

FIG. 1. Experimental setup.

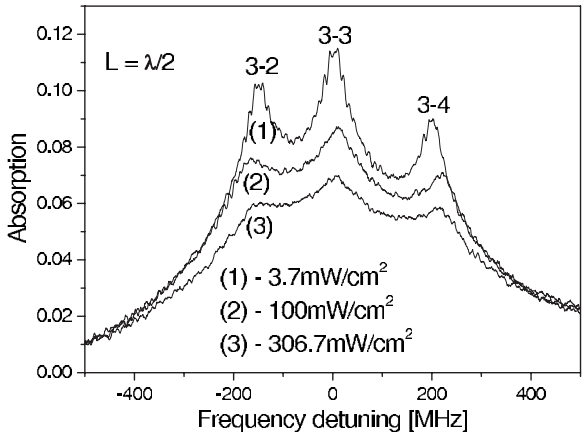

FIG. 2. Absorption spectra across the $F_g=3\rightarrow F_e=\{2,3,4\}$ transitions for various intensities (as indicated) at $L=\lambda/2$.

mission with reflection signals [11] because the nonresonant reflection vanishes for these cell lengths. The study is performed on the D_2 line of Cs vapor, with a spectral resolution about an order of magnitude better than in [7], and with an irradiation intensity orders of magnitude larger than in previous experiments on Cs vapor in an ETC [6,7]. In addition to the known occurrence of narrow dips over a broader background in the absorption spectrum [7,12], we discuss here the appearance of narrow dips over the (sub-Doppler) fluorescence spectrum. Such dips of reduced fluorescence were only briefly described in preliminary reports [12]. Here we present experimental and theoretical studies aimed at the clarification of the origin of the observed narrow dip in the fluorescence profile. An interesting peculiarity of the observed narrow reduced-fluorescence dip is that it appears for all hfs components but the one that does not suffer population loss due to hyperfine and Zeeman optical pumping.

In spite of the complexity of the Cs atomic system with respect to saturation effects (as due to the many hyperfine and Zeeman substates), we show, numerically as well as on the basis of general theoretical arguments, that the major features of our observations can be interpreted in the frame of a two-level model provided that closed and open atomic systems are distinguished.

II. EXPERIMENTAL SETUP

A scheme of the experimental setup is presented in Fig. 1. An extended cavity diode laser (ECDL) is used, performing frequency-tunable single-mode operation at $\lambda=852$ nm, with a full width at half maximum (FWHM) of about 3 MHz. The main part of the laser beam, linearly polarized, is directed at normal incidence onto the ETC. The geometry of the experiment is chosen in a way that the laboratory magnetic field (about 0.5 G) is approximately parallel to the laser light polarization. The construction of the ETC, filled with Cs vapor from a side arm, is similar to the one described in [4]. Its design was slightly modified to produce a wedge in the vapor gap. This makes the cell thickness locally variable in a convenient manner. The situations $L=\lambda/2$ or $L=\lambda$ are chosen by simply adjusting the relative position of the laser beam and of the ETC. The accuracy of the cell thickness measurement is better than 20 nm. The Cs vapor density ($\sim 4\times 10^{13}$ atoms cm^{-3}) is controlled by the temperature T of the side arm (unless stated otherwise, $T=119$ °C). The irradiating beam has a diameter of 0.4 mm. Its intensity is controlled with neutral density filters F_1. The transmitted light power is measured by the photodiode $PD1$. To ensure a constant sensitivity of the detector, the off-resonance intensity falling onto $PD1$ is kept constant by filters F_2. To record fluorescence spectra, the photodiode $PD2$ collects the induced fluorescence emitted in a direction normal to the laser beam. The spectra can be recorded either directly or through the demodulation [with a phase-sensitive detection (PSD)] of a FM applied to the laser. Auxiliary laser beams allow the monitoring of the laser frequency: (i) one beam is sent to a scanning Fabry-Perot interferometer to monitor (by means of $PD4$) the single-mode operation of the ECDL; (ii) the second one is used for an auxiliary saturated absorption (SA) setup with a macroscopic (3-cm long) Cs cell ensuring an accurate reference when scanning the ECDL frequency.

III. EXPERIMENTAL RESULTS

A. Sub-Doppler resonances in absorption

The absorption spectra comprise two sets of hfs components (a component being defined as optical transition between hyperfine substates) $F_g=3\rightarrow F_e=\{2,3,4\}$ and $F_g=4\rightarrow F_e=\{3,4,5\}$. They are represented in all the following figures through the $\Delta P/P_0$ ratio (denoted as absorption), where ΔP is the absorbed power and P_0 is the input power. The relative uncertainty on the transmission $(P_0-\Delta P)/P_0$ is on the order of a few 10^{-3}.

Figure 2 illustrates the behavior of the absorption spectrum on a cell of thickness $L=\lambda/2$, for three different irradiating intensities and for the $F_g=3\rightarrow F_e=\{2,3,4\}$ set of transitions (a similar behavior is observed for the $F_g=4\rightarrow F_e=\{3,4,5\}$ transitions). For all intensities, the enhancement of the absorption at the center of the hyperfine transitions is responsible for a strong narrowing of the spectrum, notably

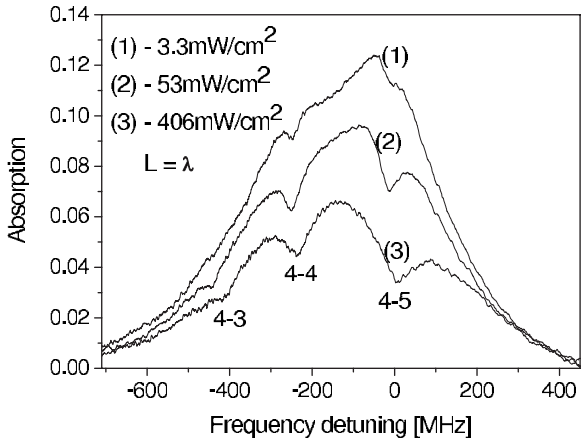

FIG. 3. Absorption spectra across the $F_g=4 \rightarrow F_e=\{3,4,5\}$ transitions for various intensities (as indicated) at $L=\lambda$.

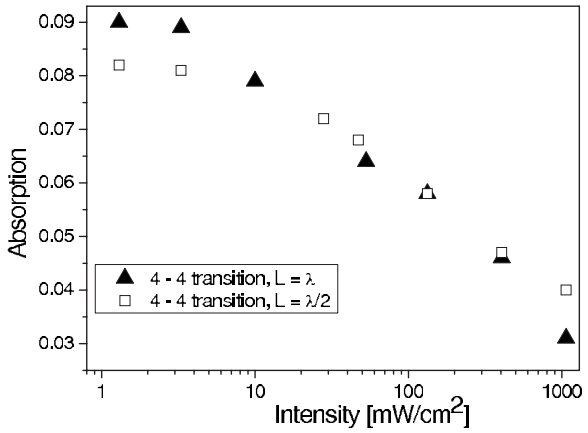

FIG. 4. Experimental absorption at the line center of the $F_g=4 \rightarrow F_e=4$ hfs component, as a function of the irradiating intensity for $L=\lambda/2$ and $L=\lambda$.

allowing the resolution of the individual hfs components. These results extend those of [6,7,12], evidencing the coherent Dicke narrowing; they are, however, obtained in an intensity range higher than the one ($\ll 1$ mW/cm^2) ensuring a genuine linear behavior. At high intensities, the sub-Doppler resonances appear significantly broadened, and saturation effects tend to washout the Dicke coherent narrowing [13], which is well-pronounced at low power: one can notice in Fig. 2 that the absorption peaks are strongly reduced for high intensities, but that the wings are nearly unaffected.

Figure 3 shows the typical evolution of the absorption spectrum for $L=\lambda$ with the irradiating intensity (only the $F_g=4 \rightarrow F_e=\{3,4,5\}$ set is shown, but a similar behavior is observed for the $F_g=3 \rightarrow F_e=\{2,3,4\}$ transitions). Significant differences are observed between the absorption spectrum at $L=\lambda/2$ and that at $L=\lambda$. Let us first recall that for $L=\lambda$, no coherent Dicke narrowing is expected, and that in the linear regime, the absorption profile, although complex, is Doppler-broad, owing to a (non-velocity-selective) transient regime of interaction. Superimposed to the expected Doppler-broadened absorption profile, one observes, as a result of the relatively high intensities used here, well-pronounced sub-Doppler narrow dips of reduced absorption. This reduction of absorption is a signature of optical pumping and/or saturation processes that tend to reduce the number of atoms available for the interaction with irradiating light. These processes can be completed only for atoms interacting a sufficient time with the laser light [1,3]: they are highly enhanced for slow atoms (i.e., small velocity component along the normal to the ETC windows), hence yielding sub-Doppler structures. The amplitude of these narrow structures increases when the irradiating intensity increases, the structures get apparently broader, and their contrast relative to the broad Doppler absorption increases markedly, as the Doppler-broadened absorption decreases under saturation. These results appear very similar to those presented for the absorption spectra in ETC of Rb vapor [12], but include a regime of a higher irradiating intensity.

Naturally, it is not a surprise that the narrow (velocity-selective) saturation dips are observed more easily when the nonsaturated line shape is broad ($L=\lambda$), than when it undergoes a notable coherent Dicke narrowing ($L=\lambda/2$). To compare more quantitatively the differing saturation behaviors for $L=\lambda/2$ and $L=\lambda$, the absorption at the center of the individual hfs component is plotted in Fig. 4 as a function of the intensity. The comparison is here restricted to the $F_g=4 \rightarrow F_e=4$ transition, but similar results are obtained for the other hfs components. It can be seen that the absorption rate decreases faster at $L=\lambda$ than at $L=\lambda/2$. This faster reduction when the length increases could be seen as reminiscent of the behavior of velocity-selective pumping already observed in micrometric thin cells [1], when the efficiency of the saturation process is governed by the product of the intensity by the cell length. An additional discussion is provided in Sec. IV.

B. Narrow resonance in fluorescence

As previously reported [4,7], the fluorescence spectra exhibit sub-Doppler features that are narrower than those in the transmitted light, with an amplitude and width following a monotonic growth with the cell thickness. Very well-resolved fluorescence spectra are recorded directly (Fig. 5) without FM and PSD of the signal. Even at low irradiation intensities [Fig. 5(a)], the signals are narrower for $L=\lambda/2$ than for $L=\lambda$. At high irradiating intensities, we observe for $L=\lambda$ tiny dips that are superimposed to the top of the fluorescence profile of the individual hfs components. Although these dips are observable through a direct detection [Fig. 5(b)], they are more conveniently characterized through the FM technique (Fig. 6). Note as an additional difference between fluorescence and absorption spectra, that these saturation dips occur for much higher irradiating intensities ($\sim$ an order of magnitude in our experiments) in fluorescence than in absorption.

To understand how these saturation features are specific to fluorescence, two major differences with absorption are worth being emphasized: (i) while the absorption rate decreases to zero under saturation effects (because the population difference is reduced), increasing the irradiating intensity tends to increase the population of the excited state, and hence the fluorescence (at least as long the atomic system is

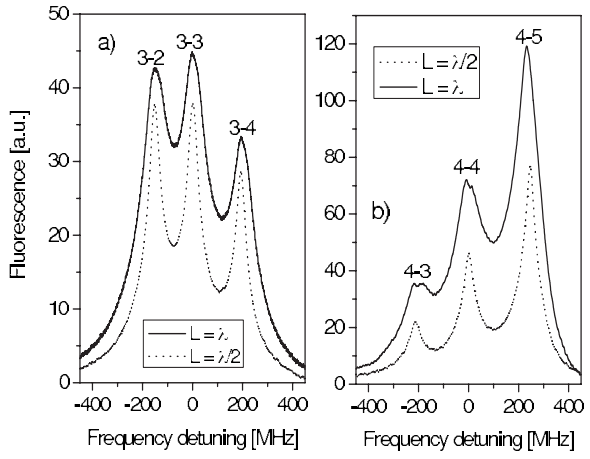

FIG. 5. Illustration of the ETC fluorescence spectra for lower (a, 7 mW/cm^2) and higher (b, 130 mW/cm^2) light intensities at the two studied cell thicknesses. Cs source temperature: 127 °C (a) and 105 °C (b).

a closed system); and (ii) even in the linear regime (i.e., low irradiating intensity), the fluorescence is a second-order process [4] that is velocity-selective in the transient regime specific to ETC. Hence the observation of narrow dips in an already narrow fluorescence spectrum can seem intriguing: in particular, for a closed atomic system, i.e., when no population loss occurs, the fluorescence rate is expected to be maximal at line center once the steady-state regime is reached. Moreover, one has to understand how a narrow velocity-selective dip of population loss can be superimposed to an already narrow velocity-selective peak of fluorescence. The last point can be tempered by the fact that the selectivity of atomic velocity decreases with increasing the cell length and is responsible for a significant broadening for lengths exceeding $\sim\lambda/2$. This makes the width of a fluorescence spectrum not as narrow as the pure natural width and this leaves open the possibility of a more selective process (population loss, assuming an open system) of the opposite sign; in addition, the sub-Doppler fluorescence spectrum already undergoes a notable broadening because of the high intensities required to observe saturation dips.

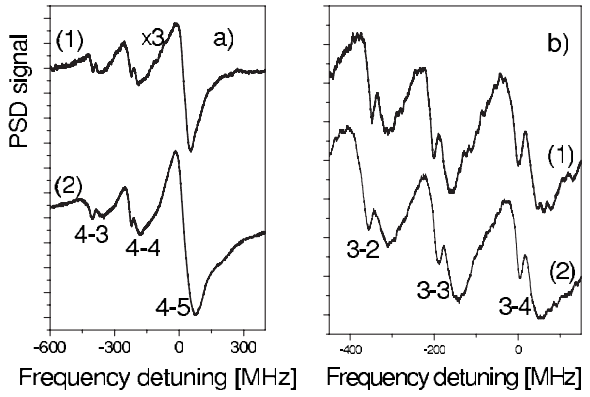

FIG. 6. PSD fluorescence spectra (for $L=\lambda$) as obtained after demodulation of an applied FM on (a) the set $F_g=4\rightarrow F_e=\{3,4,5\}$, recorded with an intensity: (1) 140 mW/cm^2 and (2) 1076 mW/cm^2, and (b) on the set $F_g=3\rightarrow F_e=\{2,3,4\}$ with an intensity: (1) 306 mW/cm^2 and (2) 800 mW/cm^2. In the PSD spectra, the narrow dispersive structure exhibits a (quasi-) antisymmetry opposed to the one of the broad structure. This is a signature of a narrow dip in the corresponding spectrum for direct detection.

Before further interpreting our experimental findings (see Sec. IV), it is interesting to point out that for the $F_g=4\rightarrow F_e=\{3,4,5\}$ set of transitions, saturation dips appear only for the open transitions $F_g=4\rightarrow F_e=3$ and $F_g=4\rightarrow F_e=4$, but are not observed for the closed transition $F_g=4\rightarrow F_e=5$ [Fig. 6(a)], in spite of the large explored range of irradiation intensities (50–1000 mW/cm^2). Conversely, Fig. 6(b) strikingly shows that for the $F_g=3\rightarrow F_e=\{2,3,4\}$ set of hfs components, all hfs components, including the closed transition $F_g=3\rightarrow F_e=2$, exhibit a comparable saturation dip in the fluorescence spectrum under the considered laser intensities. Actually, it is known that due to the Zeeman degeneracy, a closed transition pumped with polarized light cannot be simply viewed as a transition on a (degenerate) two-level system. It is in particular not protected against the Zeeman optical pumping that modifies the tensorial orientation of the hyperfine sublevel through the excitation with linearly polarized light [14]. As a result of a strong irradiation on the $F_g=3\rightarrow F_e=2$ transition, Cs atoms accumulate into the $m_F=\pm 3$ Zeeman sublevels, which do not interact with the laser light: although the transition is a closed one (in terms of energy level), a strong irradiation induces a decreased fluorescence because the system is actually an open one when considering the Zeeman degeneracy. At the opposite, on the $F_g=4\rightarrow F_e=5$ transition, Cs atoms accumulate on Zeeman sublevels with the largest absorption probability [15,16], and a strong irradiation does not reduce the fluorescence.

IV. DISCUSSION AND INTERPRETATION WITH THEORETICAL MODELING

A. Limits in interpretation and expectations from previous two-level models

Although we describe a single-laser experiment, a fully quantitative prediction would be very complex to obtain. This is because when dealing with saturation problems for a degenerate two-level system, the Rabi frequency of an elementary transition between Zeeman components depends on geometrical Clebsh-Gordon type coefficients, so that a single parameter of saturation can hardly be defined. Moreover, here, the saturation process is governed by a transient regime, and the duration of the interaction is velocity-dependent. This mixture of velocity-dependent transient regime, and of the velocity integration, justifies that several regimes have already been analyzed in the elementary frame of a nondegenerate two-level model. In all cases, the theoretical treatment of spectroscopy in a thin cell of dilute vapor assumes wall-to-wall atomic trajectory [1–3,9,13,17,18] and the optical response results from a spatial integration of the local atomic response that is determined through a transient evolution.

For relatively long cells, an elementary treatment of saturation was developed [1,3] (for an early independent ap-

proach, see [18]), relying basically on an open two-level model. Saturation effects were considered to be much slower than the coherent absorptive response, assumed to be instantaneous. They induce a velocity-selective dip in the absorption spectrum. An elementary scaling law was found, with the key parameter (the pumping time) determined by the product "cell length by pumping intensity." Even in this simplifying modeling, the identification of the atomic velocities contributing to the signal [3] has revealed to be quite complex because of an interplay between the velocity width associated to the natural optical width and the maximal velocity allowing a quasisteady state pumping.

For lower intensities and/or smaller cell length, the optical pumping remains negligible, and an elementary (closed two-level) model has to be considered [2]. The relevant transient regime is the buildup of the absorbing properties of the vapor, i.e., of the optical coherence. The interference between the various velocity-dependent (complex) coherent response of all atomic velocities is at the origin of the Dicke narrowing at $L=\lambda/2$ [and of its periodical revivals at $L=(2n+1)\lambda/2$]. The Bloch vector model [7] is an adequate tool to explain the periodical Dicke narrowing for absorption and it can be applied beyond the limits of the linear regime [19,20], or to accommodate the population losses of an open system. For a strongly driven irradiation, and a moderate relaxation (closed system), the global process remains purely coherent, but requires the velocity integration (or interference) of quickly rotating Bloch vectors. Through the interference of these multiple oscillations, it can be inferred [19,20] that varying the detuning (i.e., changing the orientation of the pseudomagnetic field in the Bloch-vector model) will lead to an oscillating behavior, instead of always yielding a maximum at line center; and indeed, a formal analytical treatment [10] for a two-level model (closed or open system) predicts such a multipeaked absorption line shape under a strong saturation, starting with a simple dip at line center for moderate saturation. However, in spite of its formal analyticity, this treatment requires a numerical determination of the relevant eigenvalues determining the solutions and becomes cumbersome for a line shape calculation. Also, no specific analysis has been provided for the situations most relevant for the coherent Dicke narrowing, only a situation close to $L=3\lambda/2$ is explicitly studied. In particular, for an open system, the problem of the competing physics of the coherent response in the saturation regime, and of the incoherent velocity-selective population depletion, has not been addressed in [10]. The systematic modeling of the fluorescence response in the context of ETC has never been reported. In [13], fluorescence spectra in ETCs are calculated, but they mostly aim at the specific description of the multilevel Rb transition.

As a further step of our study, we propose a numerical evaluation of the response of an elementary nondegenerate two-level atomic system (conservative or open two-level system), and we compare it with the experimental findings.

B. Two-level modeling in view of a numerical estimate

We consider here a two-level model with a control parameter allowing one to compare the situation of an open system

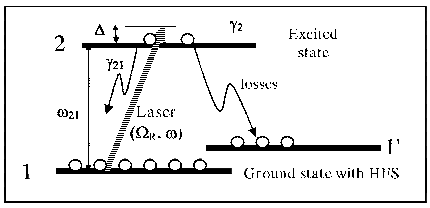

FIG. 7. Schematics of the atomic system used in the theoretical modeling.

(with losses to a generic "third level" $1'$), or of a closed system (Fig. 7). Levels 1 and 2 are coupled by a laser light at a frequency ω, detuned by Δ from the transition frequency ω_{21} ($\Delta=\omega-\omega_{21}$). The Rabi frequency is defined as $\Omega_R=2\mu_{12}E_0/\hbar$ (E_0 being the light field input amplitude) with μ_{12} the dipole moment of the transition. The width of the excited state is denoted by γ_2, and one assumes, for the considered dilute vapor, that collisions—notably dephasing collisions—can be neglected, so the optical width of the transition γ_{21} is $\gamma_{21}=\gamma_2/2$. Practically, this simple hypothesis introduces a set of dual relaxation constants. This unfortunately leads to hardly tractable analytical solutions, while the assumption of a single relaxation constant for population and optical coherence would have greatly simplified the calculations. However, such a simplifying assumption can hardly be justified in the context of an ETC, with the wall-to-wall atomic trajectories [21]. To take into account the possibility of population losses to a third level (e.g., to the other hyperfine sublevel of the ground state of alkali-metal atoms, or to the Zeeman sublevels), one introduces a coefficient, defined as α, for characterizing the probability to decay from level 2 to level 1 ($\alpha=1$ for a closed system, $0\leqslant\alpha<1$ for an open system).

The system of Bloch equations is hence the following:

$$v\frac{d\sigma_{21}}{dz}+D_{21}\sigma_{21}-i\frac{\Omega_R}{2}(\sigma_{11}-\sigma_{22})=0, \tag{1}$$

$$v\frac{d\sigma_{22}}{dz}+\gamma_2\sigma_{22}-\Omega_R\,\mathrm{Im}\,\sigma_{21}=0, \tag{2}$$

$$v\frac{d\sigma_{11}}{dz}-\alpha\gamma_2\sigma_{22}+\Omega_R\,\mathrm{Im}\,\sigma_{21}=0, \tag{3}$$

where $D_{21}=\gamma_{21}+ikv-i\Delta$, v is the atomic velocity (along the laser beam, and hence along the normal to the ETC), and the σ_{ij} are the reduced density matrix elements in the rotating frame. The above system had been solved analytically [1], in an approach focusing only on the nonlinear incoherent processes. This could be justified in view of solving the restricted problem for cell lengths allowing transient coherent processes to be negligible. Here we consider both coherent and incoherent processes that are altogether essential for the submicron sized cells.

As usual in a thin cell, the initial conditions for the system of Eqs. (1)–(3) differ for arriving ($v<0$) and departing ($v>0$) atoms. One has indeed [$\sigma_{11}(L)=1$; $\sigma_{22}(L)=0$; $\sigma_{21}(L)$

$=0]$ for $v<0$; and $[\sigma_{11}(0)=1;\ \sigma_{22}(0)=0;\ \sigma_{21}(0)=0]$ for $v>0$. To relate the solution of the system (1)–(3) to the signals of absorption or fluorescence observed in the experiments, we further follow the approach presented in [9]. The local atomic response (at z) is deduced from the integration of its transient behavior (owing to $z=vt$, or $z=L+vt$, for, respectively, $v>0$ and $v<0$). The optical signal results from the spatial integration of the atomic response, after the required integration over the velocity distribution (assumed to be a Maxwellian, with a thermal velocity u). Hence the absorption is proportional to a quantity

$$A=\int_0^\infty G(v)\exp\left[-\left(\frac{kv}{ku}\right)^2\right]dv \tag{4}$$

with

$$G(v)=\int_0^L \mathrm{Im}[\sigma_{21}(z,v)]dz. \tag{5}$$

In the experiment, the measured signal is the coherent beating between the input field and the reemitted field $I_t \sim 2E_0E_t^*$, so that it is the experimental ratio of absorption $\Delta P/P_0$ which has to be compared with the theoretical quantity A/Ω_R (or I_t/P_0). In a similar way, the fluorescence is related to the quantity U, with

$$U=\int_0^\infty Q(v)\exp\left[-\left(\frac{kv}{ku}\right)^2\right]dv, \tag{6}$$

where $Q(v)$ is defined as

$$Q(v)=\int_0^L [\sigma_{22}(z,v)]dz. \tag{7}$$

On this theoretical basis, it is possible to spatially and velocity-integrate the solutions of the density matrix equations to be found numerically under the conditions of saturation. Relatively to the previous calculations [1–3], one should recall that: (i) the modeling of the coherent Dicke narrowing was achieved on the basis of similar density matrix equations [2,17], in the limit of a first-order interaction with the resonant light (in such a case, the parameter α, affecting population redistribution, plays no role in this first order prediction, and the Bloch vector model applies), and that (ii) for the velocity-selective optical pumping in thin cells ($L \gg \lambda$) [1], the optical coherence yielding the absorption rate was estimated under a rate equation approach, allowing the instantaneous measurement of the remaining active population difference (for $\alpha \leqslant 1$).

In view of discussing some of the theoretical predictions with parameters applicable to an elementary and realistic case, the above model has been used with the following parameters: $\gamma_{21}=5$ MHz, $ku=250$ MHz, and $\alpha=1$ (closed system) or $\alpha=0.5$ for a realistic open alkali system. Technically, our numerical results combine a velocity integration, the spatial integration of a locally varying response [see Eqs. (5) and (7)], and a Runge-Kutta integration equivalent to the integration of the transient response governing the spatial response for a given velocity.

C. Comparison between model and experiments: Absorption behavior

When attempting to compare quantitatively the experimental results with a modeling, and especially if it is not intended to go to a complete line-shape analysis, it is necessary to recall various intrinsic limitations affecting the possibility of a quantitative comparison between the experiment and the above two-level model. First, this comparison remains in principle of a limited scope because multiple Zeeman transitions are involved. This means that in principle, saturation effects cannot be accounted for by converting the experimental intensity into a single Rabi frequency Ω_R. The tensorial structure of the atomic system makes nonidentical the various transfer rates to the individual sublevels. On the experimental side, the hyperfine components are not perfectly resolved, but partially overlap, moreover, in a nonconstant manner that depends upon the cell length and the saturation. This makes it uneasy to attribute all of the measured absorption at a given frequency—on the center of a hfs component, or elsewhere, to a single hfs component. This limitation is even stronger for the smallest components because they are observable only over the slope of a stronger component, adding an extra difficulty to characterize the appearance of an inverted dip structure. A rigorous measurement for a given hyperfine component would imply to subtract the contribution from the neighboring components. Such an evaluation cannot be very precise, and it becomes natural to concentrate the study on the stronger transitions. One can also mention that the uncorrected transverse structure of the irradiating intensity (presumably Gaussian) tends to wash out the tiny oscillations that could be induced by saturation [10], and that the residual terrestrial magnetic field, although not sufficient to generate a resolved Zeeman structure, may modify the coupling rates between sublevels.

For all of the above reasons, the interplay between numerous processes, with differing time constants, makes hopeless the characterization of the complex broadening of line shapes by a "width" of resonance. This is why, in an attempt to simply evaluate the onset of the appearance of a narrow inverted structure (i.e., reduced absorption), we compare predictions for an irradiation frequency at line center, and for a slightly shifted frequency (we take $\Delta=0.08ku$, or 20 MHz for numerical values as mentioned in Sec. IV B). Such a criterion, possibly misleading if the spectrum would include numerous oscillations, seems reasonable with respect to the apparent width of the various saturation dips that we observe. Figures 8–10 allow a comparison between the experimental and the theoretical results for the $F_g=4 \rightarrow F_e=4$ and $F_g=4 \rightarrow F_e=5$ transitions. These two transitions are good examples of open and closed transitions, and the corresponding "saturating intensity" (although the concept is, as mentioned, of a limited scope for a degenerate system) should be quite comparable. To make the theoretical predictions directly comparable to the experiments, we use a conversion factor $(\Omega_R/\gamma_{21})^2=1$ for 15 mW/cm^2 which was chosen to provide the most satisfactory visual fit between the experimental and theoretical curves. Also, in these figures, the absorption rate for the theoretical curves was adjusted (by a factor of 1.8) to provide the optimal comparison with the experiments; note,

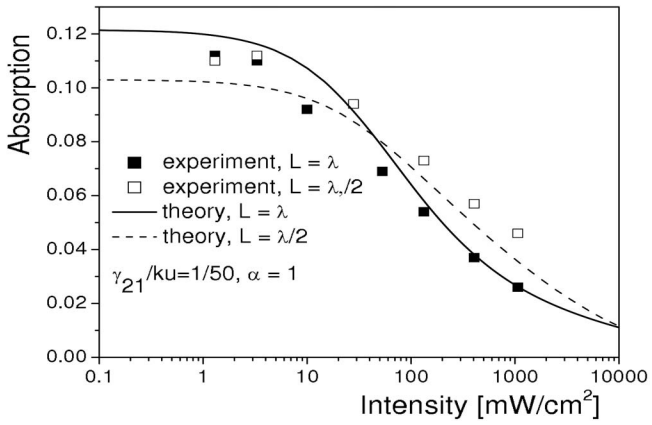

FIG. 8. Intensity dependence of the absorption—at line center—for a closed transition. The theoretical dependence for $L=\lambda/2$ is a dashed line, the solid line is for $L=\lambda$. The experimental data ($L=\lambda/2$: open squares and $L=\lambda$: closed squares) are for the closed $F_g=4\rightarrow F_e=5$ transition. For the scale applied to the theoretical curves, see text.

however, that in principle, the absorption rate is predictable in an absolute manner provided that the atomic density and the dipole moment are known.

This comparison between the simplified modeling and the experimental observations shows a satisfactory agreement. In particular, in Fig. 8, where the predicted absorption at line center is plotted in the two typical cases $L=\lambda/2$ and $L=\lambda$, one notes as predicted that if the absorption at $L=\lambda/2$ is only slightly smaller than for $L=\lambda$ for low intensities (as expected due to the Dicke narrowing, the exact ratio being governed by the γ_{21}/ku factor), the absorption becomes even larger for $L=\lambda/2$ than for $L=\lambda$ at higher intensities. Interestingly, such a result is valid for a closed system (Fig. 8) as well as for an open system—see Fig. 9. Although the saturation processes for $L=\lambda$ that reduce absorption of slow atoms are in principle twice more efficient than the comparable processes for $L=\lambda/2$, the dominant effect seems here to be the survival of the coherent Dicke narrowing (for $L=\lambda/2$), with its large contribution of fast atoms that are nearly insensitive to the saturation. This larger contribution at line center is the distinctive evidence of the coherent Dicke narrowing, induced by the coherent transient contribution of atoms that are not "slow." It is hence natural that the Dicke coherent narrowing remains quite robust, as unaffected by relatively strong irradiating intensities. However, it cannot be concluded that a narrow saturation dip in the absorption would not be observed in the conditions allowing for a revival of the Dicke narrowing, such as $L=3\lambda/2$ (a length unfortunately not attainable because of the construction of our cell): indeed, in most experimental conditions, the revival of the Dicke narrowing [6,7] (although shown to be robust with saturation at $L=3\lambda/2$, see [12]) only brings a sub-Doppler structure of a small amplitude.

Figures 9 and 10 allow the comparison of the $L=\lambda/2$ and $L=\lambda$ situations, with respect to the appearance of a narrow dip of reduced absorption, for closed and open systems. For the closed system considered in Fig. 10, one predicts [Fig. 10(b)] for $L=\lambda$ that the initially broad peak—i.e., no Dicke narrowing—exhibits an inverted substructure even for low intensities (a few mW/cm^2). Conversely, for $L=\lambda/2$ [Fig. 10(a)], the narrow Dicke structure undergoes only a visible broadening, but without the clear appearance of a dip in the center of the transition. A closer look at the inset of Fig. 10(a) shows, however, that $\Delta=0$ is no longer the peak of absorption for high intensity, but the amplitude of the corresponding dip is predicted to be extremely small. This demonstrates that the absence of observation of a narrow dip for $L=\lambda/2$ is not some fundamental effect, but rather the quantitative result of the competition between distinct processes affecting optical coherences (Dicke narrowing) or atomic population (saturation). An analogous behavior is predicted for an open system (Fig. 9, $\alpha=0.5$), with saturation at line center and a tiny dip for $L=\lambda/2$ at high intensities (slightly more pronounced than for the closed system), and the occurrence of a pronounced narrow dip for $L=\lambda$. For $L=\lambda$, the dip amplitude is predicted to be significantly larger for the open transition than for the closed one which is not observed in the experiment. For these discrepancies, it should, however, be kept in mind that our analysis here tackles narrow details

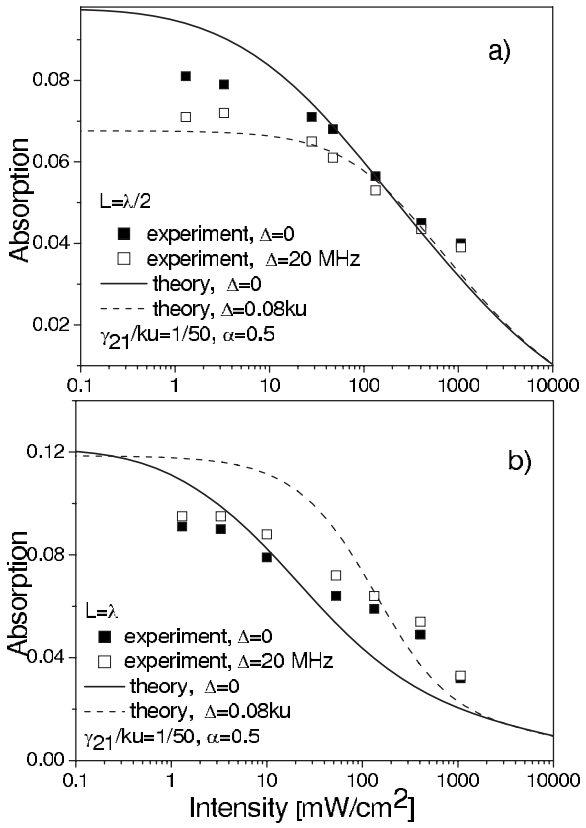

FIG. 9. Comparison between the intensity dependence of the absorption on a open transition, at line center, and at a slightly detuned frequency. The ETC thickness is (a) $L=\lambda/2$ and (b) $L=\lambda$. The theoretical dependence is shown as a solid line for a frequency at line center $\Delta=0$, and as a dashed line for a detuned frequency $\Delta=0.08ku$. The experimental data ($\Delta=+20$ MHz: open squares and $\Delta=0$: closed squares) are for the open $F_g=4\rightarrow F_e=4$ transition. For the scale applied to the theoretical curves, see text.

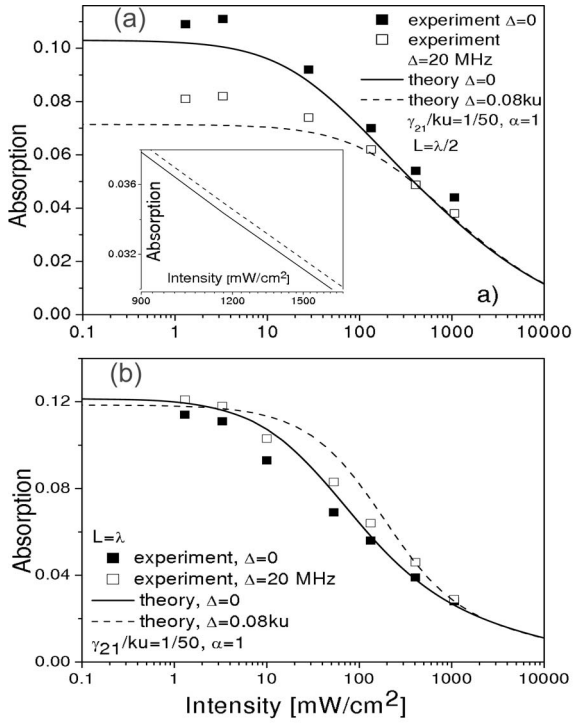

FIG. 10. Same as Fig. 9, but for a closed transition. Experimental data are for the closed $F_g=4 \rightarrow F_e=5$ transition.

of the line shapes, and that a shift of 20 MHz is experimentally small.

D. Predictions for fluorescence behavior

Because saturation effects in fluorescence are observed for higher intensities than in absorption, and mostly in a PSD technique following an applied FM, we have not attempted to perform a quantitative comparison between the experiments and the predictions of the modeling.

The numerical calculations confirm the experimental observation that line shapes are expected to be narrower in fluorescence than in absorption in comparable conditions [4,7,13]. Also, the width of the fluorescence profile is expected to increase continuously with the cell thickness, without an interferometric Dicke-type narrowing, and to reach a Doppler-broadened line shape for longer cells with the velocity selection getting less stringent. The simulation in Fig. 11 (i.e., calculation with the relevant experimental parameters) does not predict the formation of a narrow dip in fluorescence for $L=\lambda/2$ and this agrees with our experiment (Fig. 5), while under the same condition, a dip in the absorption is predicted. If such an absence of a dip can be expected for a closed system, a strong irradiation should be able to induce a severe depletion of the fluorescent atoms for an open system, and hence a dip in the line shape. However, in the sense of the dip formation, our simulation does not show essential differences between the closed and open transitions (Fig. 11). Most probably this is because for our choice of γ_{12}/ku parameter this strong irradiation would imply for $L=\lambda/2$ such a large broadening of the transition that the

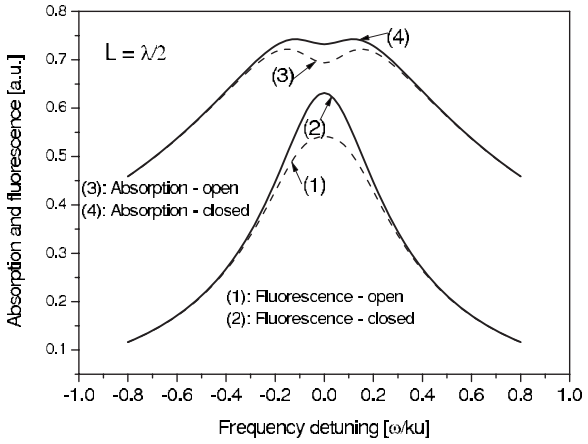

FIG. 11. Calculated fluorescence (1,2) and absorption (3,4) profiles for open (1,3) and closed (2,4) transitions under conditions where reduced absorption dip is predicted: $\Omega_R/\gamma_{12}=8$.

velocity-selection itself is governed by a width not markedly narrower than the one of the total signal.

When increasing the cell length to $L=\lambda$, Figs. 12(a) and 12(b) show, with a presentation similar to the one used in Figs 9 and 10, that a pronounced dip of reduced fluorescence at line center is predicted at $L=\lambda$ for the open transition. For a closed transition, no dip is predicted, and rather, the line shape broadens with saturation. In addition, theoretical fluorescence profiles are presented in Fig. 12(c), showing completely different behavior of the fluorescence around the transition center for the open and closed transitions. This striking theoretical difference between the closed and open system justifies our experimental observations (Sec. III B and Fig. 5), where a fluorescence dip is observed for all components but the $F_g=4 \rightarrow F_e=5$ transition.

V. CONCLUSIONS

In spite of the apparent simplicity of single beam experiments on ETCs, we demonstrate a large variety of regimes in the study of saturation. This is because thin cell spectroscopy naturally yields a signal averaged on various regimes of transient interaction between an atomic velocity group and a resonant irradiation. This also explains that a large variety of modelings has been proposed to deal with these effects. As long as the real system of an alkali atom (such as Cs in our case) is far from being a two-level system, owing to its degenerate multilevel nature and including the tensorial structure responsible for the various Zeeman substates, it is hopeless to describe in full detail the saturation effects: this can be easily understood by recalling that for alkali vapor, there exists no general description of saturated absorption spectra under a strong pump irradiation: this latter problem is, however, notably simpler as being limited to a steady state interaction, but similarly sensible to the many coupling strengths involved in the highly complex sub-Doppler atomic structure of alkali atoms. In this context, it becomes clear that an exact quantitative description would be an enormous task of a probably limited benefit. Nevertheless, it is remarkable that a

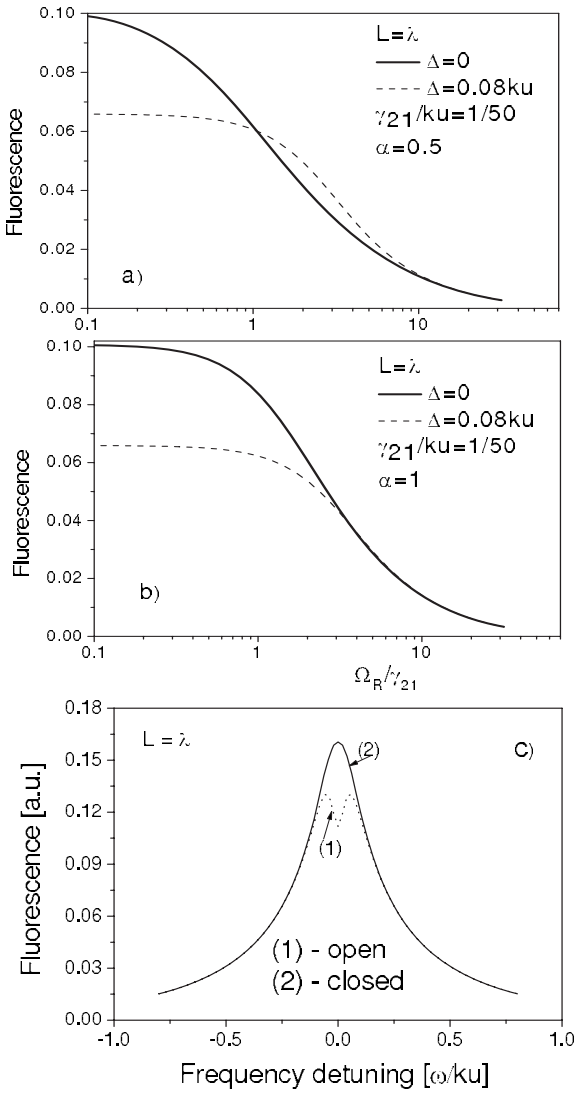

FIG. 12. Theoretical features of fluorescence for $L=\lambda$. Intensity dependence of the fluorescence (normalized by the Rabi frequency, i.e., plot of U/Ω_R^2) at line center $\Delta=0$ (solid line), and at a slightly detuned frequency $\Delta=0.08ku$ (dashed line) for (a) an open transition and (b) a closed transition. (c) Theoretical line shapes for open (1) and closed (2) transitions for $\Omega_R/\gamma_{21}=2$.

comparison between a pure two-level model, with well-chosen numerical parameters, and our experiments, leads to a relatively satisfactory agreement.

On more general grounds, some major features can be deduced from our studies. In absorption, the saturation reduces preferentially the contribution of slow atoms. This leads to the observation of saturation dips on line centers that are observed more easily when the (nonsaturated) absorption is broad (i.e., for $L=\lambda$), than when the coherent Dicke narrowing makes the line shape intrinsically narrow. For $L=\lambda/2$, the Dicke narrowing is so robust that we only observe a broadening, without the occurrence of the predicted tiny saturation dip. Because of the coherent nature of absorption processes in ETCs, the observed dips at line centers can result from the combined velocity-selective depletion of population difference and from a complex oscillating behavior. These oscillations are probably more efficient for ETC thickness leading to a coherent narrow Dicke structure, than for lengths multiple of $L=\lambda$, characterized by destructive interferences across the Doppler-broad structure, and for closed systems rather than for open systems (as characterized by an incoherent velocity-selective population transfer).

In fluorescence, it is only for open atomic systems, allowing a reduced contribution of slow atoms, that dips at line center can be observed as originating from a velocity-selective process. Also, increasing the cell length makes easier the observation of a narrow structure inside the sub-Doppler fluorescence spectrum as due to the increased width of the nonsaturated fluorescence spectrum. For effective closed systems (i.e., including the redistribution among the Zeeman sublevels), it is not clear if the fluorescence spectrum can involve oscillations, reminiscent of the kind of fringes that are predicted to appear in the absorption spectrum. This possibility could strongly depend upon the relative relaxation of the optical coherence rate, and population losses. In our experiments, the relatively strong coherence losses, owing to the relatively high Cs temperature, and the uncontrolled spatial distribution of the irradiating beam, could be sufficient reasons to make unobservable saturation features more complex than an elementary dip.

The reported results enhance our knowledge in the rich field of the Doppler-free ETC spectroscopy which is of significant importance for the development of high-resolution spectroscopy of atoms and molecules confined in nanovolumes. ETC spectroscopy has recently been shown to allow the spatial analysis of the long-range van der Waals atom-surface attraction that modifies spectra for short ETC thicknesses [22]. The recent observation [23] of electromagnetically induced transparency effect in ETC is promising for the dynamics study of this widely used phenomenon. ETC application has been proposed [24] for magnetic field measurements with submicrometer spatial resolution which can be useful for detailed magnetic mapping performance.

ACKNOWLEDGMENTS

The work was supported by the INTAS South-Caucasus Project (Grant No. 06-1000017-9001), by the French-Bulgarian Rila collaboration (French Grant No. 98013UK, Bulgarian Grant No. 3/10), by the National Science Fund of Bulgaria (Grant No. F-1404/04) and enters into the goal of the FASTnet consortium (EU support HPRN-CT-2002-00304). We appreciate the help of K. Koynov with the numerical modeling. D.S and T.V. would like to acknowledge ANSEF for the financial support (Grant No. PS-nano-657).

[1] S. Briaudeau, D. Bloch, and M. Ducloy, Europhys. Lett. **35**, 337 (1996).
[2] S. Briaudeau, S. Saltiel, G. Nienhuis, D. Bloch, and M. Ducloy, Phys. Rev. A **57** R3169 (1998).
[3] S. Briaudeau, D. Bloch, and M. Ducloy, Phys. Rev. A **59**, 3723 (1999).
[4] D. Sarkisyan, D. Bloch, A. Papoyan, and M. Ducloy, Opt. Commun. **200**, 201 (2001).
[5] R. H. Romer and R. H. Dicke, Phys. Rev. **99**, 532 (1955).
[6] G. Dutier, A. Yarovitski, S. Saltiel, A. Papoyan, D. Sarkisyan, D. Bloch, and M. Ducloy, Europhys. Lett. **63**, 35 (2003).
[7] D. Sarkisyan, T. Varzhapetyan, A. Sarkisyan, Yu. Malakyan, A. Papoyan, A. Lezama, D. Bloch, and M. Ducloy, Phys. Rev. A **69**, 065802 (2004).
[8] D. Sarkisyan, T. Becker, A. Papoyan, P. Thoumany, and H. Walther, Appl. Phys. B: Lasers Opt. **B76**, 625 (2003).
[9] G. Dutier, S. Saltiel, D. Bloch, and M. Ducloy, J. Opt. Soc. Am. B **20**, 793 (2003).
[10] H. Tajalli, S. Ahmadi, and A. Ch. Izmailov, J. Opt. B: Quantum Semiclassical Opt. **4**, 208 (2002).
[11] Note, however, that if the "reflection-like" (dispersive) component in the transmission is eliminated for $L=n\lambda/2$ (n integer), the field structure inside the ETC (see Ref. [9]) is not a running plane wave; rather, its amplitude exhibits a maximum at $z=(2n+1)\lambda/4$ that signs the (partially) standing wave nature of the field inside the ETC. This nonconstant field amplitude is in principle susceptible to affect the saturation behavior, but the spatial averaging intrinsic to the ETC response makes this effect quite marginal.
[12] T. Varzhapetyan, D. Sarkisyan, L. Petrov, C. Andreeva, D. Slavov, S. Saltiel, A. Markovski, and S. Cartaleva, Proc. SPIE **5830**, 196 (2005); D. Sarkisyan, T. Varzhapetyan, A. Papoyan, D. Bloch, and M. Ducloy, Proc. SPIE **6257**, 625701 (2006).
[13] G. Nikogosyan, D. Sarkisyan, and Yu. Malakyan, J. Opt. Technol. **71**, 602 (2004).
[14] Note that the Zeeman tensorial orientation of the sublevel does not require an external magnetic field, but is a signature of the nonisotropic nature of an atom with angular momentum. Practically, residual magnetic fields are not compensated in the experiment and are susceptible to induce a more intricate behavior, at least quantitatively, see Ref. [1].
[15] K. A. Nasyrov, Phys. Rev. A **63**, 043406 (2001).
[16] F. Renzoni, C. Zimmermann, P. Verkerk, and E. Arimondo, J. Opt. B: Quantum Semiclassical Opt. **3**, S7 (2001).
[17] B. Zambon and G. Nienhuis, Opt. Commun. **143**, 308 (1997); see also T. A. Vartanyan and D. L. Lin, Phys. Rev. A **51**, 1959 (1995).
[18] A. Ch. Izmailov, Laser Phys. **2**, 762 (1992); **3**, 507 (1993); Opt. Spectrosc. **74**, 25 (1993); **75**, 395 (1994).
[19] I. Hamdi, P. Todorov, A. Yarovitski, G. Dutier, I. Maurin, S. Saltiel, Y. Li, A. Lezama, T. Varzhapetyan, D. Sarkisyan, M.-P. Gorza, M. Fichet, D. Bloch, and M. Ducloy, Laser Phys. **15**, 987 (2005).
[20] I. Maurin, P. Todorov, I. Hamdi, A. Yarovitski, G. Dutier, D. Sarkisyan, S. Saltiel, M.-P. Gorza, M. Fichet, D. Bloch, and M. Ducloy, J. Phys.: Conf. Ser. **19**, 20 (2005).
[21] Dephasing collisions do not necessarily affect atomic trajectories, and the coherent Dicke narrowing has been demonstrated for various atomic densities, i.e., with optical width possibly much larger than the natural width as defined by the half of the inverse lifetime of the excited state.
[22] M. Fichet, G. Dutier, A. Yarovitsky, P. Todorov, I. Hamdi, I. Maurin, S. Saltiel, D. Sarkisyan, M.-P. Gorza, D. Bloch, and M. Ducloy, Europhys. Lett. **77**, 540001 (2007).
[23] A. Sargsyan, D. Sarkisyan, and A. Papoyan, Phys. Rev. A **73**, 033803 (2006).
[24] D. Sarkisyan, A. Papoyan, T. Varzhapetyan, K. Blush, and M. Auzinsh, J. Opt. Soc. Am. B **22**, 88 (2005).